

Optical light curve of GRB 121011A: a textbook for the onset of GRB afterglow in a mixture of ISM and wind-type medium

Li-Ping Xin, Jian-Yan Wei, Yu-Lei Qiu, Jin-Song Deng, Jing Wang and Xu-Hui Han

Key Laboratory of Space Astronomy and Technology, National Astronomical Observatories, Chinese Academy of Sciences, Beijing 100012, China; xlp@nao.cas.cn

Received 2015 May 1; accepted 2015 June 9

Abstract We report the optical observations of GRB 121011A by the 0.8m TNT facility at Xinglong observatory, China. The light curve of the optical afterglow shows a smooth and featureless bump during the epoch of ~ 130 s and ~ 5000 s with a rising index of 1.57 ± 0.28 before the break time of 539 ± 44 s, and a decaying index of about 1.29 ± 0.07 up to the end of our observations. Moreover, the X-ray light curve decays in a single power-law with a slope of about 1.51 ± 0.03 observed by XRT onboard *Swift* from 100 s to about 10 000 s after the burst trigger. The featureless optical light curve could be understood as an onset process under the external-shock model. The typical frequency has been below or near the optical one before the deceleration time, and the cooling frequency is located between the optical and X-ray wavelengths. The external medium density has a transition from a mixed stage of ISM and wind-type medium before the peak time to the ISM at the later phase. The joint-analysis of X-ray and optical light curves shows that the emissions from both frequencies are consistent with the prediction of the standard afterglow model without any energy injections, indicating that the central engine has stopped its activity and does not restart anymore after the prompt phase.

Key words: gamma-ray bursts — stars: individual (GRB 121011A)

1 INTRODUCTION

Gamma-ray bursts (GRBs; see e.g., Piran 2005, for a review) are the brightest flashes in the universe. Based on the duration of prompt emission in high energy, GRBs are classified into two groups: long- and short-GRBs. Long-duration GRBs are thought to be related to the death of massive stars (e.g., Xin et al. 2011). The circumburst medium density near the location of a long-duration burst might be wind-type (e.g., Dai & Lu 1998; Chevalier & Li 2000; Panaitescu & Kumar 2002; Starling et al. 2008). Multi-wavelength afterglows could be detected for almost half of GRBs when a relativistic jet sweeps into the environment medium. Comparisons of optical and X-ray light curves show that their evolutions are usually different (Panaitescu et al. 2006; Huang et al. 2007a; Xin et al. 2012; De Pasquale et al. 2015). For some bursts like the naked-eye burst GRB 080319B, they are likely to be generated by different outflows (Racusin et al. 2008). Optical light curves show a diverse behavior at the early phase (Kann et al. 2011), which could be produced by several types of radiations. If there is only forward shock emission, the brightness in low frequencies (e.g., optical, infrared, radio) is predicted to increase over time at the first phase and then decrease at the later epoch after enough medium is swept by the forward shock (Sari & Piran 1999). This kind of

process is named onset of the afterglow which usually has a peak time of about 500 s post burst (Liang et al. 2013).

The onset process was reported in some bursts (e.g., Molinari et al. 2007; Huang et al. 2012), thanks to the fast slew capability of the *Swift* satellite and quick multi-wavelength follow-up observations by ground-based telescopes. In those reports, other radiations from reverse shock, internal shock or others were detected in optical or X-ray light curves. For example, the variation in the optical light curve of GRB 060607 (Molinari et al. 2007) at the later phase was detected. During X-ray observations, flares (e.g., Burrows et al. 2005) or emissions in the steep decay phase which is related with the internal-shock process were detected (e.g., Zhang 2007; Huang et al. 2012). Recently, Li et al. (2015) found that in 87 well sampled and simultaneously observed GRBs, only nine GRBs match the prediction of the standard fireball model, and have a single power law decay in both energy bands during their entire observations. Some relationships are also investigated among different physical parameters like the isotropic energy, peak time, etc. (e.g., Liang et al. 2010; Panaitescu & Vestrand 2011; Panaitescu et al. 2013).

In this work, we report a new ideal case of the onset process in optical afterglows of GRB 121011A which was observed by the 0.8m Tsinghua University - National Astronomical Observatory of China Telescope (TNT), lo-

cated at Xinglong observatory, China. Both optical and X-ray light curves during our observation epoch have no pollution from other radiations. Thus it is an example of the “purest” case that demonstrates the onset process.

The multi-wavelength observations and data reduction are reported in Section 2. The light curve and spectral energy distribution of the afterglow are presented in Section 3. Section 4 gives the analysis and discussions. Section 5 gives the summary.

2 HIGH-ENERGY OBSERVATION AND DATA REDUCTION

At 11:15:30 UT, the *Swift* Burst Alert Telescope (BAT) triggered and located GRB 121011A. The light curve of prompt emission shows a single peak starting at -9 s and ending at about 150 s after the burst trigger. The burst duration T_{90} (15–350 keV) is 75.6 ± 12.7 s (Stamatikos et al. 2012). The *Swift* X-ray Telescope (XRT) and Ultraviolet and Optical Telescope (UVOT) began observing the burst at 97.5 s and 150 s after the burst, respectively. Follow-up observations were made by several ground-based telescopes, like the MITSuME 50 cm telescope (Kuroda et al. 2012, GCN 13846) and MASTER (Yurkov et al. 2012, GCN 13848).

The XRT light curve and spectral data were obtained from the XRT light curve and spectral repository (Evans et al. 2007, 2009). The XRT spectrum has been regrouped to ensure at least 3 counts per bin using the *grppha* task from XSPEC12.

2.1 TNT Observations

A follow-up observation campaign of GRB 121011A was carried out using the 0.8m TNT facility at Xinglong observatory. TNT is equipped with a PI 1300×1340 CCD and filters in the standard Johnson Bessel system. The observation of the optical transient of GRB 121011A was carried out with TNT beginning at 114 seconds post the *Swift*/BAT trigger and *W* and *R*-band images were obtained.

Data reduction was carried out following the standard routine in the IRAF¹ package, including bias and flat-field corrections. Dark correction was not performed since the temperature of the CCD that was used was cooled down to -110 °C. Point spread function photometry was applied via the DAOPHOT task in the IRAF package to obtain the instrumental magnitudes. During the reduction, some frames were combined in order to increase the signal-to-noise ratio. Absolute calibration was performed using several nearby stars in the USNO B1.0 R2mag. The data of GRB 121011A obtained in this work are reported in Table 1.

¹ IRAF is distributed by NOAO, which is operated by AURA, Inc., under cooperative agreement with NSF.

Table 1 Optical Afterglow Photometry Log of GRB 121011A by TNT. The reference time T_0 is the *Swift* BAT burst trigger time. “ $T - T_0$ ” is the middle time in seconds. “Exposure” is the exposure time in seconds. “Merr” means the uncertainty of magnitude. All data are calibrated by the USNO B1.0 reference stars in R2 mag. None of the data are corrected for Galactic extinction (which is $E_{B-V} = 0.03$, Schlegel et al. 1998).

$T - T_0$	Exposure	Filter	Mag	Merr
145	60	<i>W</i>	18.544	0.131
215	60	<i>W</i>	17.908	0.056
274	40	<i>W</i>	17.582	0.093
330	60	<i>W</i>	17.490	0.043
390	40	<i>W</i>	17.122	0.042
416	20	<i>W</i>	17.057	0.093
462	20	<i>W</i>	16.975	0.043
485	20	<i>W</i>	17.040	0.042
508	20	<i>W</i>	16.951	0.037
551	40	<i>W</i>	17.014	0.029
587	60	<i>R</i>	16.988	0.038
666	60	<i>R</i>	17.019	0.034
746	60	<i>R</i>	17.127	0.035
824	60	<i>R</i>	17.222	0.040
903	60	<i>R</i>	17.214	0.039
982	60	<i>R</i>	17.315	0.042
1061	60	<i>R</i>	17.427	0.055
1218	60	<i>R</i>	17.445	0.050
1297	60	<i>R</i>	17.612	0.051
1376	60	<i>R</i>	17.565	0.062
1455	60	<i>R</i>	17.806	0.062
1533	60	<i>R</i>	17.913	0.087
1612	60	<i>R</i>	17.866	0.071
1691	60	<i>R</i>	17.905	0.065
1770	60	<i>R</i>	17.970	0.082
1848	60	<i>R</i>	17.803	0.075
1927	60	<i>R</i>	18.238	0.124
2006	60	<i>R</i>	18.052	0.084
2085	60	<i>R</i>	18.331	0.116
2165	300	<i>R</i>	18.416	0.061
2483	300	<i>R</i>	18.506	0.068
3119	300	<i>R</i>	18.976	0.102
3437	300	<i>R</i>	19.276	0.133
3755	300	<i>R</i>	19.037	0.127
4073	300	<i>R</i>	19.227	0.145
4391	300	<i>R</i>	19.242	0.133
4709	300	<i>R</i>	19.581	0.213
5027	300	<i>R</i>	19.397	0.225
5345	300	<i>R</i>	19.367	0.314

3 TEMPORAL PROPERTIES OF MULTI-BAND AFTERGLOWS AND SPECTRAL ENERGY DISTRIBUTION

Figure 1 shows the optical and X-ray light curves for GRB 121011A. The reports from GCN Circular (Fynbo et al. 2012, GCN 13856; Malesani et al. 2012, GCN 13853) after the TNT observation epoch are collected in order to get larger coverage of light curves. All these magnitudes that were reported were re-calibrated by the same stars with USNO B1.0 R2 mag. The well sampled *R*-band light curve in this work during the epoch of ~ 100 s and 5400 s post burst was well fitted by a broken power-law

$$F = F_0 \left[\left(\frac{t}{t_b} \right)^{\omega\alpha_1} + \left(\frac{t}{t_b} \right)^{\omega\alpha_2} \right]^{-1/\omega}. \quad (1)$$

The temporal decaying indices are changed from $\alpha_{O1} = -1.57 \pm 0.28$ to $\alpha_{O2} = 1.29 \pm 0.07$ with a break time t_b of 539 ± 44 s and a smoothness parameter w of 1.13 ± 0.34 . The χ^2 is 50.4 with 36 degrees of freedom. The smoothness parameter w is similar to the results of GRB 060604 and GRB 060607A (Molinari et al. 2007). We also note that these values are smaller than those of most bursts (Liang et al. 2010, 2013).

During a similar observation epoch as the optical one, an X-ray light curve could be fit well with a single power law $f \sim t^{-\alpha}$ with a temporal decay index of $\alpha_{x1} = 1.51 \pm 0.03$. The χ^2 is 26.8 with 20 degrees of freedom.

Figure 2 shows the spectral energy distribution from optical to X-ray afterglows of GRB 121011A in the time interval [3000 s, 4000 s] post burst. The spectral index of X-ray was obtained as $\beta_x = -1.1 \pm 0.65$ after fitting the data with a model of a single power law ($f_\nu \sim \nu^\beta$) plus absorption due to the interstellar medium (ISM) including molecules and grains. The uncertainty in β_x is relatively large. This is because the data in the fitting region are sparse. However, regardless of the uncertainty, these optical data are located below the extrapolation of the X-ray spectral emission.

4 ANALYSIS AND DISCUSSION

4.1 Estimate the Redshift

Redshift is one of the essential parameters for constraining the properties of a burst. However, there is no specific report about the redshift of GRB 121011A in the literature. For the following analysis, we try to restrict the redshift based on multi-wavelength observations in the literature, especially in the blue band. According to the reports by Holland & Racusin (2012), during a similar epoch observed by UVOT onboard *Swift*, a successful detection of about 19.67 ± 0.07 mag was obtained in blue band u , while upper limits of 20.9, 22.6 and 21.0 mag were only given by more bluer filters of $uvw1$, $uvm2$ and $uvw2$ respectively. Assuming that the failure of afterglow detection for $uvw1$ band is caused by the Ly α forest, but the u filter is not, the Ly α absorption line would be estimated in the region of $2600 < 1216(1+z) < 3465$, which conversely makes the redshift be in the region of [1.13, 1.84], considering the central wavelengths of u (3486 Å) and $uvw1$ (2600 Å) (Roming et al. 2005). For simplicity, the redshift of 1.5 is adopted in our discussion in the next sections, which does not affect much of the main conclusions in this work.

4.2 Test with the Standard Forward Shock Model

An interesting signature for the afterglow of GRB 121011A is that the chromatic behavior during the early phase in which the optical emission is rising while X-ray emission has been in the deceleration phase. According to the forward shock synchrotron model, electrons accelerated in the shock emit synchrotron radiation. As the fireball slows down, the synchrotron peak frequency progressively

moves to a lower frequency. The optical light curve of the forward-shock emission is expected to show an initial rise with an index of -0.5 to the peak, and is then followed by a normal decay ($\alpha \sim 1$). For the case of GRB 121011A, the index in the rising phase is larger than 0.5 (Zhang et al. 2003; Wang et al. 2008), and no rebrightening exists in the following decay phase. All these properties indicate that the typical frequency has moved to the optical band ($\nu_m \leq \nu_o$) before the peak time observed in the light curve (Type III case in Jin & Fan 2007) of about ~ 539 s.

For the case of GRB 121011A, the decay index of the optical afterglow after 539 s post burst is 1.29 ± 0.07 , while that of the X-ray light curve is 1.51 ± 0.03 during the same epoch. The difference in decay indices between optical and X-ray afterglow is about 0.22, which is consistent with the case of $\nu_o < \nu_c < \nu_X$ in the ISM under slow cooling and without any injection in the frame of the standard forward shock model (Zhang et al. 2006; Gao et al. 2013), where ν_c is the cooling frequency of synchrotron radiation. This scenario is also consistent with the result in Figure 2 that optical flux is smaller than the prediction of X-ray emission, regardless of the uncertainty in the spectral slope β_x . If this were the case, the electrical energy index p would be estimated to be about 2.68 with the relationship $p = (4 \times \alpha_x + 2)/3$.

4.3 Constraining the Circumburst Medium before the Deceleration Phase

Long-duration GRBs are thought to be related to the deaths of massive stars, which indicates that the environment around the bursts would not be ISM but rather a wind-type-like medium. Within the standard forward shock model, the slopes in the rising and decaying phases of an afterglow onset depend on the circumburst medium density profile parameter k in the profile of $n = n_0(R/R_t)^{-k}$ (Liang et al. 2013), where $n_0 = 1 \text{ cm}^{-3}$, R_t is the transition radius at which the medium changes into a constant density ISM from a wind-type medium. In the spectral regime of $\nu_m < \nu_o < \nu_c$ and $p > 2$, the rising slope α is predicted to be a constant value of 3 for the ISM case (e.g., Sari & Piran 1999; Huang et al. 2007b), and it will be a varying value with the relation of $\alpha = (p - 1)/2$ for the wind model. With the estimation of $p \sim 2.68$, the α would be deduced to be $(2.68 - 1)/2 = 0.84$. The predicted values in both ISM and wind cases are not consistent with the rising value for the case of GRB 121011A.

Considering the circumburst medium density profile parameter k in the thin-shell forward-shock model (Liang et al. 2013), it gives a rising index $\alpha = -3 + k(p + 5)/4$. For GRB 121011A, the parameter k is deduced to be about 1.3 with the values of $\alpha = -1.51$ and $p = 2.68$ which are estimated above by analysis of the decaying part. This result shows that at the early epoch before the deceleration time, the medium density is a mixture of ISM and wind-type medium.

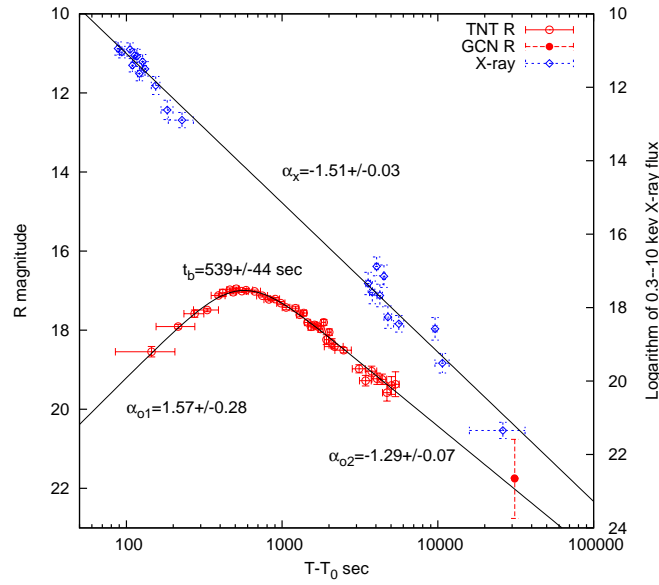


Fig. 1 The optical and X-ray afterglow light curves of GRB 121011A. Red data show the R -band light curve observed by the TNT facility, and are calibrated by USNO B1.0 R2 mag. Blue data show the X-ray light curve. All X-ray data are transformed by applying $-12-2.5 \times \log_{10} f$ for clarity of comparison.

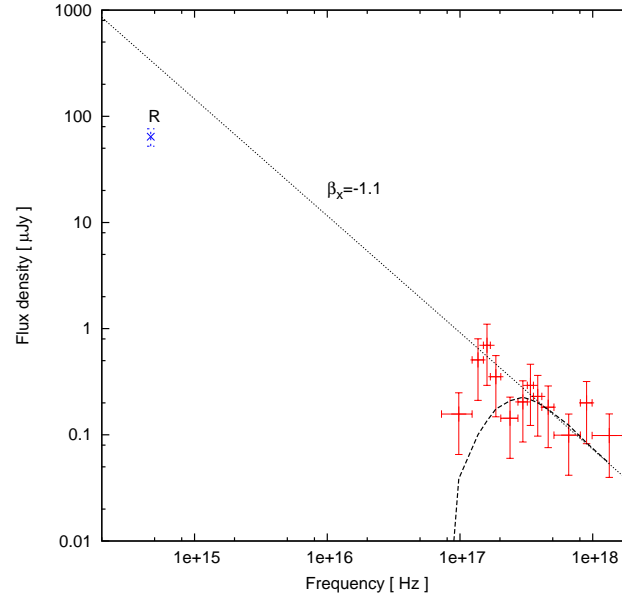


Fig. 2 Optical to X-ray spectral energy distribution of GRB 121011A in the time interval [3000 s, 4000 s] post burst. The optical one is corrected for Galactic extinction. The black dashed line shows the best fit for the X-ray emission, and the black dotted line shows the extrapolation for the spectral index ($f_\nu \sim \nu^\beta$) of X-ray emission.

4.4 No Signatures of Reverse Shock and Long Lasting Central Engine Activity

According to the standard relativistic fireball model, reverse shocks are expected to radiate emissions in the long wavelength bands in optical, infrared and radio with short bright optical flashes (e.g., Akerlof et al. 1999) and/or intense radio afterglows (e.g., Kulkarni et al. 1999) by executing a synchrotron process in a particularly early af-

terglow phase (e.g., Kobayashi & Sari 2000). The non-detection of a reverse-shock in the optical band of GRB 121011A could be classified as the type-III case (Jin & Fan 2007). The lack of an optical flash is naturally explained in the standard model if the typical frequency of the forward shock emission is lower than the optical band $\nu_m < \nu_o$ at the onset of afterglow, as discussed in Section 4.3. At the peak time, the forward and reverse shocked regions have the same Lorentz factor and internal energy density.

The cooling frequency of the reverse shock is equal to that of the forward shock. The matter density in the reverse shocked region is much higher than in the forward shock region, making the electron temperature lower. The typical frequency of the reverse shock is therefore much lower than that of the forward shock (e.g., Kobayashi & Zhang 2003; Mundell et al. 2007; Melandri et al. 2010). Another possibility for the lack of optical flash is that all the emission is produced in a magnetically dominated outflow (Jin & Fan 2007; Zhang et al. 2003).

In the *Swift* era, the behavior of X-ray emission at the early phase is very complex. High latitude prompt emission (the first steep decay phase) and flares in the early epoch are observed in most bursts (e.g., Chincarini et al. 2010), which are thought to be related to the central engine activity. The shallow-decay phase (or plateau phase) in the canonical light curve (e.g., Zhang et al. 2006) is also considered to be caused by energy injection (Dai & Lu 1998, 2000; Fan & Xu 2006; Yu & Huang 2013) from long-lasting central engine activity or other sources (for a review, see Zhang 2007). Unlike most bursts reported before, GRB 121011A shows a single decay during all of its X-ray observations. No steep decay phase, flares or shallow-decay phase is observed as early as the beginning of the observation at $t \sim 100$ s, indicating that the central engine stops its activity at ~ 100 s post its initial burst. The emission related to the prompt emission must decay very rapidly from a very early time. Furthermore, the central engine does not restart anymore at the later phase.

4.5 The Onset Process and Constraining the Initial Lorentz Factor

The smooth and featureless light curve in the optical afterglow of GRB 121011A is clearly consistent with the prediction of the onset process when the relativistic jet meets the medium in the environment around the burst (e.g., Sari & Piran 1999; Kobayashi & Zhang 2007). Since the break time of about 539 s post burst from the rise part to the decay one in the optical light curve, the peak time would be inferred to be $t_p = t_b(-\alpha_{o1}/\alpha_{o2})^{1/[w(\alpha_{o2}-\alpha_{o1})]} \sim 572 \pm 50$ s following the estimation of Molinari et al. (2007). The peak time t_p is larger than the duration of high-energy prompt emission of about 100 s, making the burst a thin-shell case. In this scenario, the quantity $t_p/(1+z)$ corresponds to the deceleration timescale $t_{\text{dec}} \sim R_{\text{dec}}/(2c\Gamma_{\text{dec}}^2)$, where R_{dec} is the deceleration radius, c is the speed of light and Γ_{dec} is the fireball Lorentz factor at t_{dec} . Therefore, initial Lorentz factor Γ_0 could be estimated since it is twice Γ_{dec} (Panaitescu & Kumar 2000).

If the environment were a homogeneous medium, the initial Lorentz factor could be estimated with the relation $\Gamma_0 \sim 193(n\eta)^{-1/8} \times (E_{\gamma,\text{iso},52}/t_{p,z,2}^3)^{1/8}$ (Liang et al. 2010). According to the joint-analysis of X-ray to optical afterglows of GRB 121011A in Section 4.3, properties of the environment around the burst do not fully agree with only ISM, since it has a distribution described with pa-

rameter $k \sim 1.3$. If considering the case of $R \sim R_{\text{dec}}$, the external medium density is $n \sim n_0 \sim 1$. Under these conditions, the estimation above for the initial Lorentz factor could be adopted, and Γ_0 is less dependent on n , η and $E_{\gamma,\text{iso},52}$. As a result, a relationship between the initial Lorentz factor and the peak time in the rest-frame was deduced by Liang et al. (2010), which was $\log \Gamma_0 = (3.59 \pm 0.11) - (0.59 \pm 0.05) \log t_{p,z}$. For the case of GRB 121011A, based on the relationship and a redshift of roughly 1.5, the peak time would be $t_{p,z} \sim 230$. If this were the case, Γ_0 can be inferred to be 157.

5 SUMMARY

The optical light curve of GRB 121011A shows a featureless bump during the epoch of ~ 130 s and ~ 5000 s with a rising index of 1.57 ± 0.28 before the break time of 539 ± 44 s, and a decaying index of about 1.29 ± 0.07 up to the end of our observations. Moreover, the X-ray light curve decays in a single power-law with a slope of about 1.51 ± 0.03 from 100 s to about 10000 s after the burst. The joint-analysis of X-ray and optical light curves after the peak time shows that the emission from both frequencies is consistent with the prediction of the standard afterglow model under the condition of ISM, and the cooling frequency is located between optical and X-ray. At the early phase, the rising index in the optical light curve is different from the predictions of the standard model under the cases of ISM and wind-type, but is consistent with the condition that the external medium is at a mixed stage of the ISM and wind-type. In addition, the typical frequency ν_m has moved to optical before the deceleration time, since there is no signature indicating the transition by ν_m from optical frequency (Jin & Fan 2007). No radiation from other mechanisms like reverse shock or those related to the internal shock are detected in either optical or X-ray light curves during all the observation epochs, making this burst the ‘‘purest’’ one for the onset of afterglows.

Acknowledgements This work was supported by the National Basic Research Program of China (973 program, 2014CB845800) and the National Natural Science Foundation of China (NSFC, Grant No. U1331202). This work made use of data supplied by the UK Swift Science Data Centre at the University of Leicester. XLP acknowledges the support from the NSFC (Nos. 11103036 and U1331101). Y. Qiu is also supported by the NSFC (No. U1231115).

References

- Akerlof, C., Balsano, R., Barthelmy, S., et al. 1999, *Nature*, 398, 400
- Burrows, D. N., Romano, P., Falcone, A., et al. 2005, *Science*, 309, 1833
- Chevalier, R. A., & Li, Z.-Y. 2000, *ApJ*, 536, 195
- Chincarini, G., Mao, J., Margutti, R., et al. 2010, *MNRAS*, 406, 2113

- Dai, Z. G., & Lu, T. 1998, *A&A*, 333, L87
- Dai, Z. G., & Lu, T. 2000, *ApJ*, 537, 803
- De Pasquale, M., Kuin, N. P. M., Oates, S., et al. 2015, *MNRAS*, 449, 1024
- Evans, P. A., Beardmore, A. P., Page, K. L., et al. 2007, *A&A*, 469, 379
- Evans, P. A., Beardmore, A. P., Page, K. L., et al. 2009, *MNRAS*, 397, 1177
- Fan, Y.-Z., & Xu, D. 2006, *MNRAS*, 372, L19
- Fynbo, J. P. U., Xu, D., Malesani, D., & Sodor, A. 2012, *GRB Coordinates Network*, 13856, 1
- Gao, H., Lei, W.-H., Zou, Y.-C., Wu, X.-F., & Zhang, B. 2013, *New Astron. Rev.*, 57, 141
- Holland, S. T., & Racusin, J. L. 2012, *GRB Coordinates Network*, 13864, 1
- Huang, K. Y., Urata, Y., Kuo, P. H., et al. 2007a, *ApJ*, 654, L25
- Huang, Y.-F., Lu, Y., Wong, A. Y. L., & Cheng, K. S. 2007b, *ChJAA (Chin. J. Astron. Astrophys.)*, 7, 397
- Huang, K. Y., Urata, Y., Tung, Y. H., et al. 2012, *ApJ*, 748, 44
- Jin, Z. P., & Fan, Y. Z. 2007, *MNRAS*, 378, 1043
- Kann, D. A., Klose, S., Zhang, B., et al. 2011, *ApJ*, 734, 96
- Kobayashi, S., & Sari, R. 2000, *ApJ*, 542, 819
- Kobayashi, S., & Zhang, B. 2003, *ApJ*, 597, 455
- Kobayashi, S., & Zhang, B. 2007, *ApJ*, 655, 973
- Kulkarni, S. R., Djorgovski, S. G., Odewahn, S. C., et al. 1999, *Nature*, 398, 389
- Kuroda, D., Yanagisawa, K., Shimizu, Y., et al. 2012, *GRB Coordinates Network*, 13846, 1
- Li, L., Wu, X.-F., Huang, Y.-F., et al. 2015, *ApJ*, 805, 13
- Liang, E.-W., Yi, S.-X., Zhang, J., et al. 2010, *ApJ*, 725, 2209
- Liang, E.-W., Li, L., Gao, H., et al. 2013, *ApJ*, 774, 13
- Malesani, D., D'Avanzo, P., Melandri, A., Nascimbeni, V., & Padilla, C. 2012, *GRB Coordinates Network*, 13853, 1
- Melandri, A., Kobayashi, S., Mundell, C. G., et al. 2010, *ApJ*, 723, 1331
- Molinari, E., Vergani, S. D., Malesani, D., et al. 2007, *A&A*, 469, L13
- Mundell, C. G., Melandri, A., Guidorzi, C., et al. 2007, *ApJ*, 660, 489
- Panaiteescu, A., & Kumar, P. 2000, *ApJ*, 543, 66
- Panaiteescu, A., & Kumar, P. 2002, *ApJ*, 571, 779
- Panaiteescu, A., Mészáros, P., Burrows, D., et al. 2006, *MNRAS*, 369, 2059
- Panaiteescu, A., & Vestrand, W. T. 2011, *MNRAS*, 414, 3537
- Panaiteescu, A., Vestrand, W. T., & Woźniak, P. 2013, *MNRAS*, 433, 759
- Piran, T. 2005, in *American Institute of Physics Conference Series*, 784, *Magnetic Fields in the Universe: From Laboratory and Stars to Primordial Structures*, eds. E. M. de Gouveia dal Pino, G. Lugones, & A. Lazarian, 164
- Racusin, J. L., Karpov, S. V., Sokolowski, M., et al. 2008, *Nature*, 455, 183
- Roming, P. W. A., Kennedy, T. E., Mason, K. O., et al. 2005, *Space Sci. Rev.*, 120, 95
- Sari, R., & Piran, T. 1999, *ApJ*, 520, 641
- Schlegel, D. J., Finkbeiner, D. P., & Davis, M. 1998, *ApJ*, 500, 525
- Stamatikos, M., Barthelmy, S. D., Baumgartner, W. H., et al. 2012, *GRB Coordinates Network*, 13852, 1
- Starling, R. L. C., van der Horst, A. J., Rol, E., et al. 2008, *ApJ*, 672, 433
- Wang, J. H., Schwamb, M. E., Huang, K. Y., et al. 2008, *ApJ*, 679, L5
- Xin, L.-P., Liang, E.-W., Wei, J.-Y., et al. 2011, *MNRAS*, 410, 27
- Xin, L. P., Pozanenko, A., Kann, D. A., et al. 2012, *MNRAS*, 422, 2044
- Yu, Y.-B., & Huang, Y.-F. 2013, *RAA (Research in Astronomy and Astrophysics)*, 13, 662
- Yurkov, V., Sergienko, Y., Varda, D., et al. 2012, *GRB Coordinates Network*, 13848, 1
- Zhang, B., Kobayashi, S., & Mészáros, P. 2003, *ApJ*, 595, 950
- Zhang, B., Fan, Y. Z., Dyks, J., et al. 2006, *ApJ*, 642, 354
- Zhang, B. 2007, *ChJAA (Chin. J. Astron. Astrophys.)*, 7, 1